Polarisation insensitive single band, dual band and broadband THz metamaterial absorbers

J.Grant[1], Y. Ma[1], Q. Chen[1], S. Saha[1], A. Khalid[1], D. R.S. Cumming[1]

[1]School of Engineering, University of Glasgow, Glasgow, G12 8LT, UK.
e-mail: james.grant@glasgow.ac.uk

Abstract

We present the design, simulation and experimental verification of single band, dual band and broadband polarisation insensitive resonant metamaterial absorbers in the THz region. All metamaterial absorbers consist of a metal/dielectric spacer/metal structure allowing us to maximize absorption by varying the dielectric material and thickness hence the effective electrical permittivity and magnetic permeability. An experimental absorption of 77% at 2.12 THz (in the operating frequency range of THz QCLs) is observed for a single band absorber while the dual band absorber has an absorption magnitude of 68% at 2.7 THz and 74% at 5.2 THz. Our broadband absorber hass greater than 40% absorption across a frequency range of 1.5-3 THz. Such efficient THz absorbers are sought in a variety of applications such as THz imaging.

1. Introduction

Since the first theoretical [1] and experimental demonstration [2] of the unique properties of metamaterials (MM) research into the topic has grown rapidly. A branch of MMs that is currently provoking wide interest is the topic of so called MM perfect absorbers. By manipulating the effective electrical permittivity, ε, and magnetic permeability, μ, absorption close to unity is possible [3]. The concept of a MM absorber is especially important at THz frequencies where it is difficult to find strong frequency selective THz absorbers. Such MM absorbers naturally lend themselves to THz detection applications, such as thermal sensors that, if integrated with suitable THz sources (e.g. QCLs), could lead to compact, highly sensitive, low cost THz imaging systems.

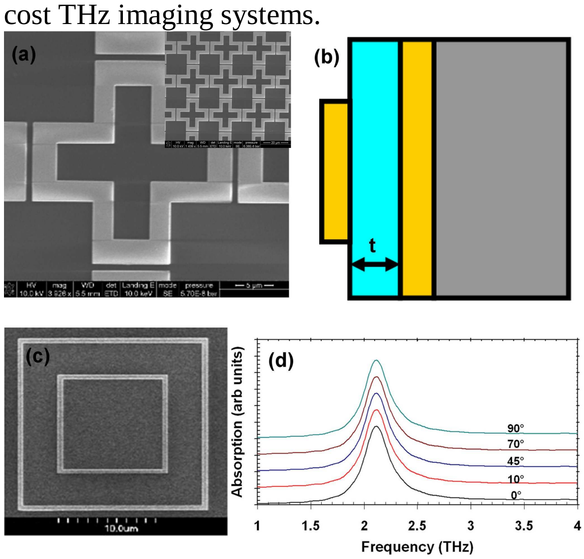

Fig. 1: (a) SEM image of a single ERR of the single band MM absorber and (b) cross-section of the complete MM absorber. (c) SEM image of the the dual band absorber. (d) Absorption spectra for different incident polarisation angles showing polarisation insensitivity of the single band MM absorber. Each successive plot from 0-90° is offset by one major unit of the ordinate axis.

The schematic of a unit cell of our single band MM absorber is shown in Fig. 1(a) and the layer cross-section is shown in Fig. 1(b). Two metallic elements, one ground plane and a cross shaped resonator, are separated by a dielectric layer of thickness, *t*. The cross-shaped resonator depicted in Fig. 1(a) is an example of an electric ring resonator (ERR) and couples strongly to uniform electric fields, but negligibly to magnetic ones. By pairing the ERR with a ground plane, the magnetic component of the incident THz wave induces a current in the sections of the ERR that are parallel to the direction of the E-field. An anti-parallel image current also flows in the region of the ground plane immediately below the cross that results in a resonant response. Significantly, the electric and magnetic response can then be tuned independently by varying the geometry of the ERR and the distance between the two metallic elements. Frequency selective narrowband THz absorbers have obvious applications in THz imaging however the realisation of multi-band absorbers would open up further THz applications such as spectroscopy. An SEM image of the ERRs that make up a unit cell of a dual band absorber is shown in Fig. 1(c). Each concentric ring is 0.5 μm wide while the inner ring has a side length of 11 μm and the outer ring a side length of 19 μm. The principle of operation is similar to that of the single band in that the concentric ring provides the electric response while the magnetic response is governed by the ring and the ground plane.

2. Simulation and Fabrication

Optimised MM absorber designs were obtained through systematic finite difference time domain (FDTD) simulations (Lumerical). The 3D simulations were performed with a plane wave source incident in the z direction on the metal/dielectric/metal/substrate unit cell. The metallic sections of the absorber were modelled as Au with a frequency independent conductivity of $4\text{x}10^7$ Sm^{-1}. Reflection and transmission spectra were recorded at planes 100 μm above and 100 μm below the ERR. The FDTD simulations revealed the absorption characteristics of the MM absorber were not sensitive to the polarisation angle of the incident EM wave (see Fig. 1(d)). Standard metal evaporation, spin coating and e-beam lithography techniques were used to fabricate devices. Full details may be found in [4].

Samples were characterized under vacuum in a Bruker IFS 66v/S Fourier Transform Infrared Spectrometer in transmission mode at normal incidence and in reflection mode at 30° incidence. The measured transmission spectra were normalized with respect to the signal measured from a 7 mm diameter open aperture and the reflection spectra were normalized to that of a gold mirror. The resulting absorption, A, was therefore calculated using $A(\omega) = 1 - R(\omega) - T(\omega)$ where R is the reflection and T the transmission. Experimental measurements were also performed on samples with no ERR layer to confirm that absorption was a consequence of the MM structure and not of the dielectric. The 8 μm thick polyimide sample with no ERR structure had a maximum absorption of 5 % across the frequency range of interest, see Fig. 2(a), thereby verifying that at the resonance frequency absorption was a result of the MM structure.

3. Results

The experimentally obtained absorption spectra as well as the simulated data for a MM absorber with a 3.1 μm thick polyimide dielectric spacer are shown in Fig. 2(a). A refractive index of 1.68 + 0.06i was used for the polyimide. The peak absorption was measured to be 77% at 2.12 THz for a polyimide thickness of 3.1 μm. This result is in excellent agreement with the simulated absorption maximum of 81%. As the polyimide thickness increases from 1 μm to 3.1 μm the peak absorption increases, but at polyimide thicknesses greater than 3.1 μm there is a slight reduction in the peak absorption value. A distinct red-shift of 0.25 THz is observed as the polyimide thickness increases from 1 μm to 7.5 μm. Absorbers that had SiO_2 as the dielectric instead of polyimide were also studied. A maximum absorption value of 65% at 1.90 THz was measured for such a MM absorber with a 3 μm thick SiO_2 dielectric layer. The effective permittivity and permeability were extracted from the simulated data via inversion of the S parameters [4]. The retrieved parameters for the simulated MM absorber with a 3.1 μm thick polyimide spacer are displayed in Fig. 2(b). As can be observed the real parts of the optical constants cross close to zero – a condition required for zero reflection, while whenever the real part of the permittivity is positive the real part of the permeability is negative and vice versa – a condition required for zero transmission.

ISBN 978-952-67611-0-7

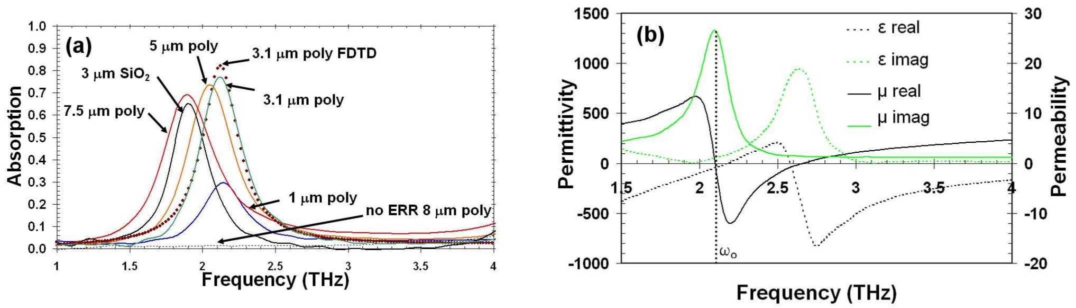

Fig. 2: (a) Experimental and simulated data of MM absorbers with differing spacer thickness and type. (b) Extracted optical parameters from the simulated 3.1 μm thick polyimide MM absorber.

Experimental and simulated absorption spectra for dual band and broad band absorbers are shown in Fig. 3(a). The dual band absorber has two absorption peaks located at 2.7 THz and 5.2 THz. The experimentally obtained absorption at these two frequencies is 64% and 74% respectively. A broad band absorber, consisting of 5 concentric rings, has greater than 35% absorption between 1.6 and 3.1 THz. The simulated power absorption distributions for the ERR, dielectric and the ground plane layers of the single band absorber are shown in Figs. 3(b-e). From these plots it is clear that the majority of the energy is dissipated as Ohmic loss in the ERR layer and as dielectric loss in the first 500 nm of polyimide below this layer.

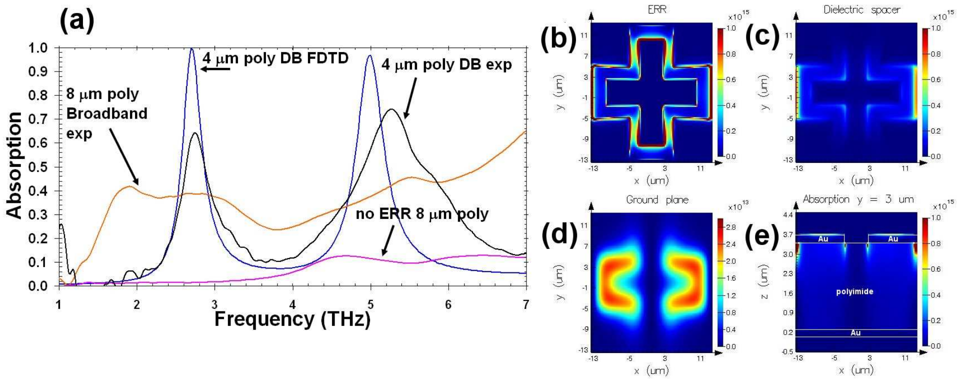

Fig. 3: (a) Absorption spectra of dual band and broad band absorbers (b-e) Simulated absorption distribution of single band absorber.

4. Conclusion

In conclusion we have demonstrated single band, dual band and broad band MM absorbers suitable for wide ranging THz applications such as THz imaging and spectroscopy. Furthermore, all MM absorbers presented here are polarisation insensitive, as a result of symmetry, maximising absorption for arbitrarily polarized light.

References

[1] J. B. Pendry, A. J. Holden, D. J. Robbins, and W. J. Stewart, "Magnetism from conductors and enhanced nonlinear phenomena," IEEE Trans. on Microwave Theory and Techniques, **47**, 2075-2084 (1999).

[2] D. R. Smith, W. J. Padilla, D. C. Vier, S. C. Nemat-Nasser, and S. Schultz, Composite medium with simultaneously negative permeability and permittivity, Phys. Rev. Lett. 84, 4184-4187 (2000).

[3] N. I. Landy, C. M. Bingham, T. Tyler, N. Jokerst, D. R. Smith, and W. J. Padilla, Design, theory, and measurement of a polarization-insensitive absorber for terahertz imaging, Phys. Rev. B **79**, 125104 (2009).

[4] Y. Ma, Q. Chen, J. Grant, S. C. Saha, A. Khalid and D. R. S. Cumming, A Terahertz polarization insensitive dual band metamaterial absorber, Opt. Lett. **36** Issue 6, 945-947 (2011)

[5] D. R. Smith, D. C. Vier, T. Koschny, and C. M. Soukoulis, Electromagnetic parameter retrieval from inhomogeneous metamaterials, Phys. Rev. E **71**, 036617 (2005).